Journal of Physics: Conference Series **2374** (2022) 012039 doi:10.1088/1742-6596/2374/1/012039

Laser spectroscopic studies of long-lived pionic helium at PSI

M. Hori[1], H. Aghai-Khozani[1,4], A. Sótér[1,5], A. Dax[2] and D. Barna[3,6]

[1] Max-Planck-Institut für Quantenoptik, Hans-Kopfermann-Strasse 1, D-85748 Garching, Germany
[2] Paul Scherrer Institut, Forschungsstrasse 111, CH-5232 Villigen, Switzerland
[3] CERN CH-1211, Geneva 23, Switzerland

E-mail: Masaki.Hori@mpq.mpg.de

Abstract. A recent laser spectroscopy experiment of three-body pionic helium atoms which was carried out using the 590 MeV ring cyclotron facility of the Paul Scherrer Institute (PSI) is briefly reviewed. The charged pion mass may be precisely determined by measuring the transition frequency of the pionic atom and comparing the results with quantum electrodynamics (QED) calculations. The experimental methods used to detect the atomic resonance are described.

1. Introduction

The PiHe collaboration recently carried out spectroscopy of metastable pionic helium ($\pi^4\mathrm{He}^+ \equiv \pi^- + {}^4\mathrm{He}^{2+} + e^-$) atoms [1–9] using a sub-nanosecond infrared laser [10, 11]. This exotic atom is made of an alpha particle, a ground-state electron, and a negatively-charged pion in a highly excited state with principal and orbital angular momentum quantum numbers of $n \approx \ell + 1 \approx 17$. The pionic orbital has a very small overlap with the atomic nucleus and so have lifetimes of nanoseconds. This enabled the first laser spectroscopy of an atom containing a meson [11]. The transition frequencies of the atom can be obtained by quantum electrodynamics (QED) calculations. By comparing the calculated and measured frequencies, the π^- mass may be precisely determined [12–14]. The experiment may also determine upper limits on the laboratory constraints on the muon antineutrino mass [15], and exotic forces that may arise between a pion and helium nucleus [16–19]. Similar experiments have been carried out on metastable antiprotonic helium ($\overline{p}\mathrm{He}^+ \equiv \overline{p} + \mathrm{He}^{2+} + e^-$) atoms at the Antiproton Decelerator of CERN [20–27]. Of particular interest is the fact that the $\pi^4\mathrm{He}^+$ atom contains no hyperfine structure due to the spin-spin interaction between the ^{4}He nucleus and pion, and so QED effects relevant to such boson-boson bound states can be precisely studied [28, 29].

[4] Present address: McKinsey and Company, Sophienstrasse 26, 80333 Munich, Germany
[5] Present address: ETH Zürich, IPA, Otto-Stern-Weg 5, 8093 Zurich, Switzerland
[6] Present address: Institute for Particle and Nuclear Physics, Wigner Research Centre for Physics, H-1525 Budapest 114, P.O.B. 49, Hungary

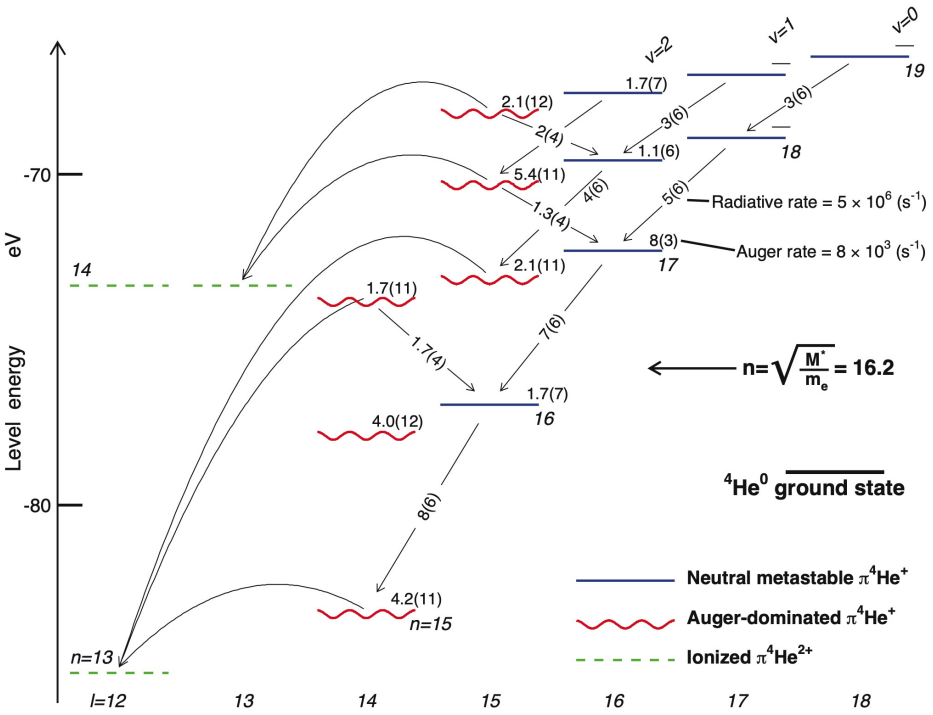

Figure 1. Energy level diagram of long-lived three-body pionic ^{4}He atoms. The energy of the states (n, ℓ) are indicated relative to the three-body-breakup threshold. Wavy lines show Auger-dominated states, solid lines states with lifetimes of > 10 ns. Auger decay rate of each state is indicated in s^{-1}. The dashed lines show the two-body ionic states that are formed after Auger emission. The curved arrows indicate Auger transitions. Radiative transitions of the type $(n, \ell) \to (n-1, \ell-1)$ and $(n, \ell) \to (n-1, \ell+1)$ are shown by arrows with the decay rates indicated in s^{-1}. From Ref. [10].

2. Experimental method

In the experiment, laser beams of pulse length $\Delta t = 800$ ps and wavelength $\lambda \approx 1631$ nm were used to excite a transition from the pionic state $(n, \ell) = (17, 16)$ that had a nanosecond-scale lifetime, to a state $(17, 15)$ with a $\tau = 5$ ps Auger lifetime and subsequent nuclear absorption [10, 30–33] (Fig. 1). The $\pi^4\mathrm{He}^+$ resonance was revealed as a peak in the rate of neutrons, protons, and deuterons that emerged from the resulting pion absorption in the nucleus. This laser resonance signal was superimposed on a background of pions that underwent immediate absorption, and $\pi^4\mathrm{He}^+$ that spontaneously decayed with a $\tau \approx 7$ ns lifetime [6, 10].

The πE5 beamline [34] provided a π^- beam of momentum $p = 83$–87 MeV/c and intensity $N_\pi = (2-3) \times 10^7$ s^{-1}. Most of the background electrons and muons in the beam was removed using a Wien filter and slit collimator. The π^- travelled through a segmented plastic scintillator plate and then entered the experimental helium target. The π^- arrived at average intervals of $\Delta t = 19.75$ ns which corresponded to the reciprocal of the $f_a = 50.63$ MHz accelerating radiofrequency of the PSI ring cyclotron. The laser beams of pulse energy $E = 10$ mJ and repetition rate of $f_r = 80.1$ Hz were produced [11] by an injection-seeded, optical parameteric generator (OPG) and amplifier (OPA) laser system (see Fig. 2 (b)). The laser beam irradiated the pionic atoms at a time $t = 9$ ns after π^- arrival. The production rate of the atoms was estimated as $> 3 \times 10^5$ s^{-1}, the probability of coincidence of a laser pulse irradiating the atom as $\approx 10^{-3}$.

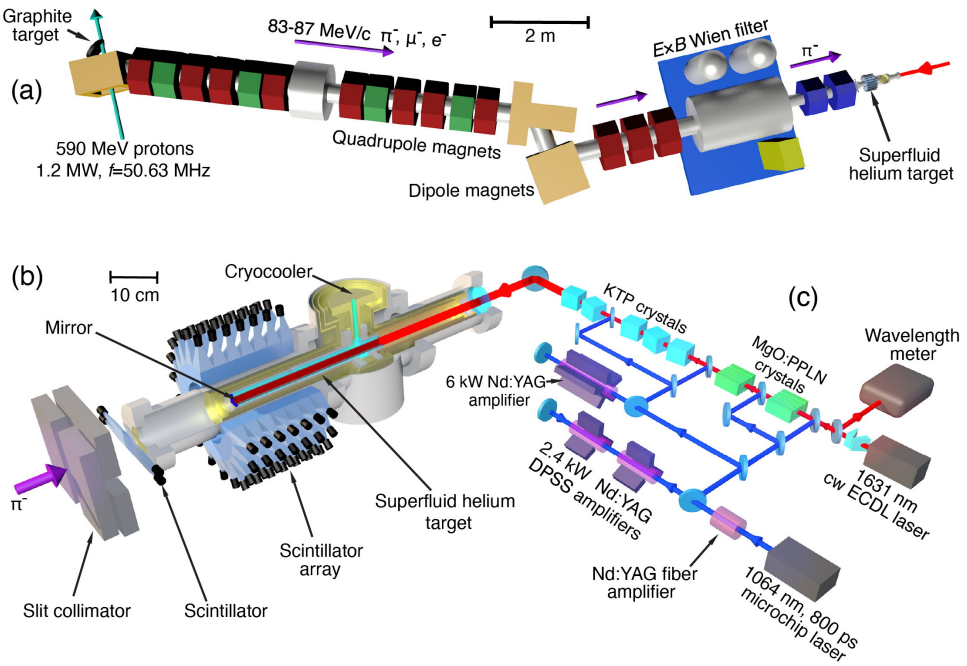

Figure 2. (a): Layout of the experimental beamline. (b): Layout of the experiment. The π^- beam travels through a segmented scintillation counter before coming to rest in the helium target. The $\pi^4\mathrm{He}^+$ atoms are irradiated with the laser pulses. The nuclear fragments that emerge from the pion absorption in the nuclei are detected by an array of scintillation counters. (b): Schematic layout of the laser system. From Ref. [11].

The signal neutrons, protons, deuterons, and tritons [10, 35, 36] had kinetic energies of a few tens of MeV. Their arrival times and energy depositions were measured by an array containing 140 plastic scintillation counters that surrounded the target. The size of the individual counters $40 \times 35 \times 34$ mm^3 was optimized to provide a $< 10\%$ detection efficiency for neutrons of energy $E \geq 25$ MeV [10]. We rejected the background electrons in the beam or those that were produced in μ^- decays, by removing the events that had small energy depositions. The waveform [37–40] of the scintillation counter signals were acquired using a data acquisition system based on the DRS4 application-specific integrated circuit (ASIC). A variant of this system was used in an experiment to measure the limits on the cross sections σ_A of antiprotons of kinetic energy $E \approx 125$ keV annihilating in target foils [39, 41, 42]. The measurements were an extension of our recent experiments using antiprotons of $E = 5.3$ MeV [40, 43–45].

3. Experimental results

The blue time spectrum of Fig. 3 (a) shows the particle arrivals at the scintillator array which were measured without laser irradiation. The sharp peaks at $t = 0$ and 19.75 ns correspond to pions that came to rest in the target that underwent prompt nuclear absorption. A $(2.1 \pm 0.7)\%$ fraction of the pions instead gave rise to a time spectrum of metastable $\pi^4\mathrm{He}^+$ that decayed with a lifetime of $\tau = (7 \pm 2)$ ns in the intervals between the π^- arrival peaks.

We searched for the transitions $(n, l) = (16, 15) \rightarrow (17, 14)$ and $(16, 15) \rightarrow (16, 14)$ using a combined dye and Ti:Sapphire [46] laser, but no significant signal was observed. We then searched for $(17, 16) \rightarrow (17, 15)$ using the OPO-OPA laser. The time spectrum indicated by filled circles superimposed in Fig. 3 (b) was measured with the OPG laser tuned to a wavelength

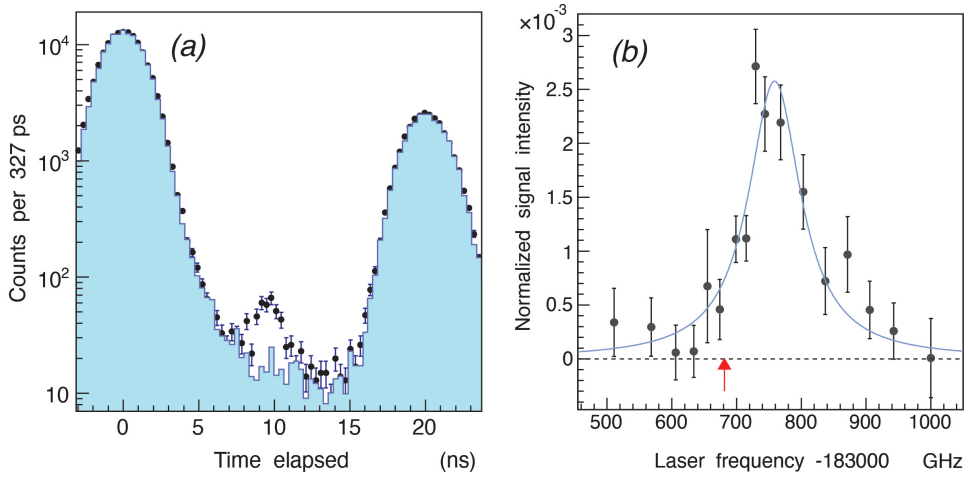

Figure 3. (a): Time spectra of nuclear fragments measured with (indicated by filled circles) and without (blue histogram) laser irradiation. The peak in the former spectrum at $t = 9$ ns is the resonance signal of $(17, 16) \rightarrow (17, 15)$. (b): Profile measured by scanning the laser over the resonance and plotting the normalized signal counts. From Ref. [11].

$\lambda \approx 1631.4$ nm. The laser-resonance peak was detected at time $t = 9$ ns. The experimental detection rate of 3 h^{-1} resonant events is compatible with the expected value from Monte Carlo simulations [10] in which most of the pionic atoms populated state $(17, 16)$. When the laser was detuned off the resonance frequency, the signal decreased and disappeared.

By scanning the laser frequency and plotting the number of resonant events, the profile shown in Fig. 3(b) was obtained. The vertical error bars indicate the statistical uncertainty of the numbers of the resonant $\pi^4\mathrm{He}^+$ events. The resonance width of ≈ 100 GHz is consistent with the Auger width $\Gamma_A = 33$ GHz of state $(17, 15)$ [10], and various contributions from collisional [8] and power broadening, and the laser linewidth. Atomic collisions that shorten [7, 47] the state lifetimes may also cause additional broadening. The best fit (blue curve) of two overlapping Lorentzian functions which take the hyperfine sublines arising from the electron spin is shown. The resonance centroid was obtained as $\nu_{\mathrm{exp}} = 183760(6)(6)$ GHz. The statistical uncertainty is 6 GHz. The systematic uncertainty of 6 GHz contains contributions related to the selection of the fit function and the uncertainty related to the laser. The measured frequency is larger than the calculated frequency $\nu_{\mathrm{th}} = (183681.8 \pm 0.5)$ GHz [10]. This is believed to be due to atomic collisions in the target that shift the atomic transition frequency [7, 8, 47, 48]. The blueshift of the frequency predicted from the impact approximation of the binary collision theory of spectral lineshapes [8] is between $\Delta\nu = 96$ and 142 GHz. This roughly agrees with the experimental result.

We intend to search for other laser transitions which should be narrower by a factor of at least 10^{-3} compared to this detected resonance [10]. Though the precision of the theoretical transition frequency ν_{th} is currently limited by the experimental uncertainty of the π^- mass, the relative precision of the calculations [10] can be improved to $< 10^{-8}$, using techniques developed for studies of HD^+ [49–51] and $\overline{p}\mathrm{He}^+$ [20, 21]. We will also carry out two-photon laser spectroscopy of $\overline{p}\mathrm{He}^+$ [52] using the new ELENA facility [53, 54] at CERN.

Acknowledgments

This work was supported by the Max-Planck-Gesellshaft and the European Science Council Starting Grant.

References

[1] Condo G T 1964 *Phys. Lett.* **9** 65
[2] Russell J E 1969 *Phys. Rev. Lett.* **23** 63
[3] Fetkovich J G and Pewitt E G 1963 *Phys. Rev. Lett.* **11** 290
[4] Block M M *et al.* 1963 *Phys. Rev. Lett.* **11** 301
[5] Zaimidoroga O A, Sulyaev R M and Tsupko-Sitnikov V M 1967 *Sov. Phys. JETP* **25** 63
[6] Nakamura S N *et al.* 1992 *Phys. Rev. A* **45** 6202
[7] Korobov V I, Bekbaev A K, Aznabayev D T and Zhaugasheva S A 2015 *J. Phys. B* **48** 245006
[8] Obreshkov B and Bakalov D 2016 *Phys. Rev. A* **93** 062505
[9] Baye D and Dohet-Eraly J 2021 *Phys. Rev. A* **103** 022823
[10] Hori M, Sótér A and Korobov V I 2014 *Phys. Rev. A* **89** 042515
[11] Hori M, Aghai-Khozani H, Sótér A, Dax A and Barna D 2020 *Nature* **581** 37
[12] Lenz S *et al.* 1998 *Phys. Lett. B* **416** 50
[13] Trassinelli M *et al.* 2016 *Phys. Lett. B* **759** 583
[14] Daum M, Frosch R and Kettle P-R 2019 *Phys. Lett. B* **796** 11
[15] Assamagan K *et al.* 1996 *Phys. Rev. D* **53** 6065
[16] Salumbides E J, Ubachs W and Korobov V I 2014 *J. Mol. Spectrosc.* **300** 65
[17] Murata J and Tanaka S 2015 *Class. Quantum Gravity* **32** 033001
[18] Ficek F *et al.* 2018 *Phys. Rev. Lett.* **120** 183002
[19] Lemos A S, Luna G C, Maciel E and Dahia F 2019 *Class. Quantum Gravity* **36** 245021
[20] Korobov V I, Hilico L and Karr J-P 2014 *Phys. Rev. Lett.* **112** 103003
[21] Korobov V, Hilico L and Karr J-P 2014 *Phys. Rev. A* **89** 032511
[22] Hu M-H, Yao S-M, Wang Y, Li W, Gu Y-Y and Zhong Z-X 2016 *Chem. Phys. Lett.* **654** 114
[23] Baye D, Dohet-Eraly J and Schoofs P 2019 *Phys. Rev. A* **99** 022508
[24] Bai Z-D, Zhong Z-X, Yan Z-C and Shi T-Y 2021 *Chin. Phys. B* **30** 023101
[25] Hori M *et al.* 2006 *Phys. Rev. Lett.* **96** 243401
[26] Hori M *et al.* 2011 *Nature* **475** 484
[27] Hori M *et al.* 2016 *Science* **354** 610
[28] Koch J and Scheck F 1980 *Nucl. Phys. A* **340** 221
[29] Trassinelli M and Indelicato P 2007 *Phys. Rev. A* **76** 012510
[30] Hori M *et al.* 2005 *Phys. Rev. Lett.* **94** 063401
[31] Sakimoto K 2009 *Phys. Rev. A* **79** 042508
[32] Zatorski J and Pachucki K 2010 *Phys. Rev. A* **82** 052520
[33] Korenman G Y and Yudin S N 2021 *Eur. Phys. J. D* **75** 64
[34] Abela R, Foroughi F and Renker D 1992 *Z. Phys. C* **56** S240
[35] Cernigoi C *et al.* 1981 *Nucl. Phys. A* **352** 343
[36] Daum E *et al.* 1995 *Nucl. Phys. A* **589** 553
[37] Ritt S, Dinapoli R and Hartmann U 2010 *Nucl. Instrum. and Meth. A* **623** 486
[38] Sótér A *et al.* 2014 *Rev. Sci. Instrum.* **85** 023302
[39] Todoroki K *et al.* 2016 *Nucl. Instr. and Meth. A* **835** 110
[40] Murakami Y, Aghai-Khozani H and Hori M 2019 *Nucl. Instrum. and Meth. A* **933** 75
[41] Aghai-Khozani H *et al.* 2012 *Eur. Phys. J. Plus* **127** 125
[42] Aghai-Khozani H *et al.* 2021 *Nucl. Phys. A* **1009** 122170
[43] Bianconi A *et al.* 2011 *Phys. Lett. B* **704** 461
[44] Corradini M *et al.* 2013 *Nucl. Instrum. and Meth. A* **711** 12
[45] Aghai-Khozani H *et al.* 2018 *Nucl. Phys. A* **970** 366
[46] Hori M and Dax A 2009 *Opt. Lett.* **34** 1273
[47] Hori M *et al.* 2001 *Phys. Rev. Lett.* **87** 093401
[48] Bakalov D, Jeziorski B, Korona T, Szalewicz K and Tchoukova E 2000 *Phys. Rev. Lett.* **84** 2350
[49] Alighanbari S, Giri G S, Constantin F L, Korobov V I and Schiller S 2020 *Nature* **581** 152
[50] Patra S *et al.* 2020 *Science* **369** 1238
[51] Hori M 2020 *Science* **369** 1160
[52] Hori M and Korobov V I 2010 *Phys. Rev. A* **81** 062508
[53] Chohan V *et al.* 2014 Extra Low ENergy Antiproton (ELENA) ring and its transfer lines: Design report Tech. Rep. CERN-2014-002 CERN, Geneva, Switzerland
[54] Hori M and Walz J 2013 *Prog. Part. Nucl. Phys.* **72** 206